

SOME PROPERTIES OF THE ATMOSPHERIC BOUNDARY LAYERFOR LOAN to
Met Office Staff only

D J CARSON

LIBRARY

(Notes prepared for the SO Course Advanced Lectures, The Atmospheric Boundary Layer, Feb 1985)

NB These notes are intended to supplement

- a. Carson, D J 1976 The Atmospheric Boundary Layer Introductory Lectures, Met O 20 Tech Note No II/84 ,
- b. SO Course Advanced Lectures, Feb 1982, The Physical Structure of the Atmospheric Boundary Layer.

1. The Physical Nature of The Atmospheric Boundary Layer

1.1 What is the atmospheric boundary layer ?

The atmospheric boundary layer (planetary boundary layer; mixing layer) is the lowest layer of the atmosphere under the direct influence of the underlying surface. Its character and depth vary in an evolutionary way in response to changes in the physical nature of the surface, the surface fluxes of sensible and latent heat, as well as changes in the 'external' synoptic field.

In the aerodynamic sense the boundary layer is simply the layer from which momentum is extracted and transferred downward to overcome surface friction. The important role played by the buoyancy forces generated by the surface heating and cooling and the presence of moisture helps distinguish the atmospheric boundary layer from the more classical laboratory boundary layers.

The formation of the atmospheric boundary layer then is a consequence of the various interactions between the atmosphere and the underlying surface.

The flow in the atmospheric boundary layer is turbulent except possibly in very stable conditions e.g. in strong inversion situations at night. The velocity, temperature, humidity and other properties in a turbulent flow can be considered as random functions of space and time and it is usually necessary to resort to a statistical approach to the calculation/prediction of boundary-layer properties. See, for example, Chap 2 of Carson(1976). In particular, this introduces the concepts of mean values, fluctuations and variances. Let s be some quantity which will fluctuate because of the turbulent motion, then

$$s = \bar{s} + s'$$

where \bar{s} is the mean value of s and s' is the turbulent or eddy fluctuation. Other essential quantities in any general statistical description of turbulent flow include :

Variance of s :

$$\sigma_s^2 = \overline{(s - \bar{s})^2} = \overline{s'^2}$$

Standard deviation of s :

$$\sigma_s = \sqrt{\overline{s'^2}}$$

Intensity of turbulent fluctuations :

$$i_s = \frac{\sigma_s}{\bar{s}}$$

A further qualitative definition of the atmospheric boundary layer is the layer extending upwards from the surface to where all turbulent flux-divergences resulting from surface action have fallen to zero (or virtually so).

Since the flux of momentum, or shearing stress, is by definition significant in this layer, it enters into the balance of forces between the pressure gradient force and the Coriolis force causing vertical shears of horizontal wind in both

magnitude and direction. The wind speed tends to fall below its free-stream (geostrophic) value found above the layer, eventually to zero at the surface although the fall-off may not always be monotonic, especially in stable conditions. The wind direction also changes with height with the biggest deviation from the geostrophic direction occurring at the surface, and whilst the deviation tends to be quite variable, influenced as it is by local topography and meso- and synoptic-scale accelerations, on average the surface wind is backed some 10° over the sea, 20° over land in unstable conditions and 30° or more in stable conditions. The resulting flow down the pressure gradient provides a significant source of momentum to balance the shearing stress at the ground and on a synoptic scale is important in generating horizontal convergence and upward motions. See, for example, Chap 3 of Carson (1976).

Sometimes the atmospheric boundary layer is capped by a well-marked inversion, generated either synoptically or by the evolutionary growth processes within the layer. Across the inversion there is usually some wind shear, a decrease in humidity and a drop in the turbulent fluxes to virtually zero (see examples in Figs 1 and 2). On other occasions, however, no clearly marked top exists and the turbulent fluxes decrease only very gradually with increasing height.

Typically the depth of the boundary layer over land evolves continuously in response to spatial and temporal changes in surface conditions. The daytime depth is typically in the range $\frac{1}{2}$ - 2 km, whereas the night-time depth is generally much shallower and in extremely stable conditions may be only a few tens of metres (see the example in Fig 3, taken from Carson(1973)).

Over land during a clear summer day convection is initiated near the surface and the flow becomes unstable and highly turbulent. As the sun sets, the air immediately in contact with the surface is cooled and becomes denser than the air above. Vertical mixing is inhibited and the flow is said to be stable. See Section 1.2 of Carson (1976).

The density stratification is unimportant only in strong-wind conditions when the sky is heavily overcast. Then the depth and structure of the boundary layer are governed by mechanical mixing generated by instabilities in the shear flow due to the effects of the surface friction. This type of boundary layer is called a neutral boundary layer.

1.2 Methods of estimating the depth of the atmospheric boundary layer.

The evolution of the daytime unstable boundary layer can often be well simulated by assuming that the surface sensible heat flux and the 'entrained' heat flux at the top of the boundary layer are distributed throughout a deepening, thermally well-mixed layer.

Fig 4 gives a schematic representation of the simple geometry of the developing convectively unstable boundary layer.

Fig 5 gives a schematic representation of the mechanisms of entrainment.

Fig 6 illustrates the success of one such simple scheme (from Carson (1973)).

Fig 7 is a practical nomogram for estimating the depth of the mixed layer in daytime conditions typical of the UK. For further details see, for example, Carson (1973) and Smith and Carson (1974).

1.3 Breakdown of the conventional atmospheric boundary layer.

The boundary layer is a region of variable character and depth which frequently acts as a buffer zone where heat, moisture, momentum and pollution are fed into it (or extracted from it) from the underlying surface and stored and accumulated until such a time that for one of various reasons the boundary layer 'breaks down' and its contents are redistributed through a much greater depth of the atmosphere.

For example :

- a. Deep penetrative convection. In the presence of convective cloud, significant vertical fluxes may continue upwards from the boundary layer as conventionally defined into the clouds whilst being very small outside at the same height. See, for example, Fig 8.
- b. Boundary-layer break-down processes occur at synoptic fronts and in the flow over mountain ranges.
- c. The continuous synoptic-scale vertical motion, aided by the diurnal cycle in the depth of the boundary layer, which 'pumps' the contents of the boundary layer upwards in the middle of the day, leaving it behind at night to be acted on by steady synoptic upward motions.

2. Properties of The Underlying Surface Which Affect The Atmospheric Boundary Layer

(Henceforth the notes apply in particular to boundary layers over land.)

2.1 Definition of the surface turbulent fluxes.

Smith and Carson (1977) contended (the somewhat oversimplified view) that over the land the surface turbulent fluxes are determined primarily by external factors independent of the details of the boundary layer and that the boundary layer adjusts its own structure in order to accommodate these inputs in the most efficient way it can. The structure does not therefore determine the inputs but is determined by them. If this philosophy is to be followed then it is worth recalling some of the external factors and surface boundary conditions that help determine and constrain the surface fluxes.

It is appropriate at this stage to identify the main surface fluxes of interest.

$\overline{w's'}$, the eddy covariance of some conservative quantity s (mean value \bar{s}) and the vertical velocity component w , represents the mean vertical turbulent flux of s at a given height.

Momentum flux (τ_o) The horizontal shearing stress at the surface, τ_o , is conventionally a vector measure of the downward flux of horizontal momentum directed parallel to the limiting wind direction as the surface is approached. Its magnitude τ_o is expressed

$$\tau_o / \bar{\rho}_o = -(\overline{w'v'})_o = \mu_*^2$$

where μ_* (defined by $\sqrt{\tau_o / \bar{\rho}_o}$) is the surface friction velocity, $\bar{\rho}_o$ is a representative mean air density near the surface.

Sensible heat flux (H_o) $H_o / \bar{\rho}_o c_p = (\overline{w'\theta'})_o = -\mu_* T_*'$

where c_p is the specific heat of air at constant pressure. The potential temperature θ is used as the temperature which is conserved in the large-scale mixing. T_* (like μ_*) is introduced as a scaling parameter defined in terms of H_o and μ_* .

Water vapour flux (E_o) $E_o / \bar{\rho}_o = (\overline{w'q'})_o = -\mu_* q_*$

where q is the specific humidity and q_* the corresponding surface scaling parameter.

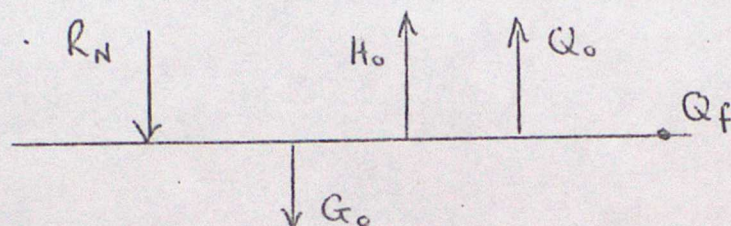
2.2 Surface roughness length and the surface boundary condition for momentum.

The surface boundary conditions for momentum transfer are :

- a. $\bar{V} = 0$ at the surface (THE NO-SLIP CONDITION)
- b. τ_o is parallel to the limiting wind direction as the surface is approached.

The magnitude of z_0 will depend, in part, on the aerodynamic roughness of the underlying surface. This property of the surface is most commonly and adequately represented by a single length, the surface roughness length, denoted z_0 . z_0 will be defined more formally later; but for now let me state that it is an empirically determined 'length' characteristic of the surface and usually independent of the flow. Typical values of z_0 range from about 10^{-4} m for a relatively smooth sea surface to about 1 m or so over a city or extensive forest. A typical value close to an extensive and uniform short-grass surface would be 1-3 cm depending on the length of the grass. Most of the standard text books on the subject will provide a table of values of z_0 for different surfaces. See, for example, Table 1 (reproduced from Panofsky and Dutton (1984)).

2.3 Land-surface temperature and heat balance.



The turbulent sensible and latent heat fluxes are components in the general balance of the energy fluxes at the surface which may be written

$$R_N = G_0 + H_0 + Q_0 + Q_f$$

where R_N = the net downward radiative flux at the surface

$$\begin{aligned} &= R_{SN} + R_{LN} \\ &= (1-\alpha) R_{S\downarrow} + \epsilon (R_{L\downarrow} - \sigma T_0^4) \end{aligned}$$

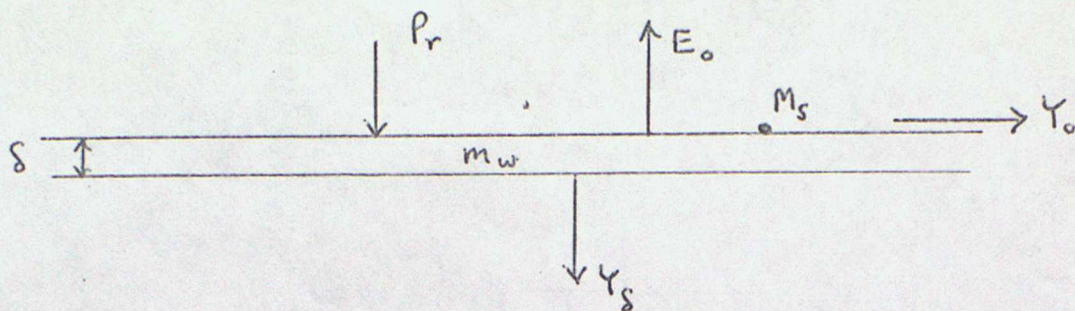
where R_{SN} is the net downward solar radiative flux at the surface,
 R_{LN} is the net downward long-wave radiative flux at the surface,
 $R_{S\downarrow}$ is the downward solar radiative flux at the surface,
 $R_{L\downarrow}$ is the downward long-wave radiative flux at the surface,
 T_0 is the surface temperature,
 α is the surface albedo,
 ϵ is the surface long-wave emissivity or absorptivity, and
 σ is the Stefan-Boltzmann constant.

$Q_0 = L_i E_0$ represents the latent heat flux due to surface evaporation or sublimation by turbulent transfer (L_i is the latent heat of evaporation, or sublimation).

$Q_f = L_f M_s$ represents the latent heat flux required to effect phase changes associated with melting or freezing at the surface, where L_f is the latent heat of fusion and M_s is the rate of snowmelt and/or icemelt.

G_0 represents a flux of sensible heat into the soil at the surface which, conventionally, is assumed to be positive when directed away from the surface into the soil. It depends on the soil's thermal properties which in turn depend on, for example, the type of surface, the type of soil and whether it is wet, dry, frozen or snow-covered, and whether it is bare soil or vegetation

2.4 Surface hydrology and the soil water budget.



The water vapour flux (i.e. the surface evaporation) E_o is also constrained by the surface hydrological state and the soil water budget. Consider the change in the soil moisture content in a single shallow surface layer of soil of depth δ . It is altered by rainfall, evaporation (condensation), snowmelt and runoff according to a water mass balance equation of the form

$$\frac{\partial m_w}{\partial t} = P_r - E_o + M_s - Y_o - Y_s$$

where m_w is the mass of liquid water per unit lateral area in the layer considered, P_r is the intensity of surface rainfall, Y_o is the intensity of surface runoff, and Y_s is the intensity of percolation out of the surface layer to lower layers.

A corresponding budget equation can be formulated for snow on the surface.

The evaporation itself depends on many factors, including the hydrological state of the surface, the spatial variability of soil type, the availability of soil moisture, the spatial and temporal variability of the vegetation, etc.

Schemes for estimating H_o and E_o should be consistent with the constraints of the surface energy balance and the surface water budget equations. An example of typical diurnal variation in the components of the surface energy balance is given in Fig 9. For further discussion see, for example, Carson (1982).

3. The Stratified Atmospheric Boundary Layer

For fuller discussion see, for example, Chap 4 of Carson (1976).

3.1 The turbulent kinetic energy balance equation.

The complete mathematical expression of the turbulent kinetic energy balance may be formed from the equations of motion of a viscous compressible fluid. If we assume that the mean flow is horizontal and that horizontal gradients can be neglected compared with vertical gradients then a simplified version of the turbulent kinetic energy balance equation is

$$\frac{\partial \bar{\epsilon}}{\partial t} = \frac{\bar{\tau}}{\bar{\rho}} \cdot \frac{\partial \bar{v}}{\partial z} - \frac{g}{\bar{\rho}} (\bar{\rho}' w') - D - \epsilon$$

where $\bar{\epsilon} = \frac{1}{2} (\overline{u'^2} + \overline{v'^2} + \overline{w'^2})$ is the mean turbulent k.e.,

$\bar{\tau} = (-\bar{\rho} \overline{u'w'}, -\bar{\rho} \overline{v'w'})$ are the Reynolds stresses,

$$\begin{aligned}
 -\frac{g}{\bar{\rho}} (\overline{\rho' w'}) & \text{, the buoyancy term of the turbulent kinetic energy balance equation,} \\
 & \approx \frac{g}{\bar{T}} \overline{w' \theta'} + 0.61 g \overline{w' q'} \\
 & = \frac{g}{\bar{\rho} c_p \bar{T}} (H + 0.61 c_p \bar{T} E) \approx \frac{g}{\bar{\rho} c_p \bar{T}} (H + 0.07 Q).
 \end{aligned}$$

Note that Q must be about 15 times larger than H to be of equal importance in the buoyancy term. This term is therefore often neglected, particularly over relatively dry land surfaces.

$$D = \frac{1}{\bar{\rho}} \frac{\partial}{\partial z} \left[\overline{w' (p' + \bar{\rho} \epsilon)} \right]$$

represents the divergence per unit mass of the vertical flux of eddy k.e. and potential energy due to the pressure fluctuations.

$$\epsilon = \nu \left\{ \left(\frac{\partial w'}{\partial z} \right)^2 + \left(\frac{\partial v'}{\partial z} \right)^2 + 2 \left(\frac{\partial u'}{\partial z} \right)^2 \right\}$$

represents the mean rate of molecular/viscous dissipation per unit mass of turbulent k.e. where ν is the kinematic viscosity.

3.2 Flux-gradient relationships.

The classical theoretical approach to the diffusion of material in turbulent flow, analogous to molecular diffusion, is to adopt a gradient-transfer approach. In this approach it is assumed that turbulence causes a net movement of material down the gradient of material concentration, at a rate which is proportional to the magnitude of the gradient. Generally, we write for the vertical turbulent transport through a horizontal plane

$$F_s = \overline{w' s'} = -K_s \frac{\partial \bar{s}}{\partial z}$$

where K_s is the eddy diffusivity or eddy diffusion coefficient. Formally we may look upon this relationship as defining K_s .

Thus our three turbulent fluxes $\bar{\epsilon}$, H , E are often expressed as

$$\begin{aligned}
 \bar{\epsilon}/\bar{\rho} &= -(\overline{w' u'}, \overline{w' v'}) = \left(K_m \frac{\partial \bar{u}}{\partial z}, K_m \frac{\partial \bar{v}}{\partial z} \right), \\
 H/\bar{\rho} c_p &= (\overline{w' \theta'}) = -K_H \frac{\partial \bar{\theta}}{\partial z}, \\
 E/\bar{\rho} &= (\overline{w' q'}) = -K_w \frac{\partial \bar{q}}{\partial z}.
 \end{aligned}$$

3.3 The Richardson Numbers.

The ratio of the production of turbulent kinetic energy due to buoyancy forces to that due to the Reynolds stresses is conventionally expressed in the form of the flux Richardson number, R_f , where

$$\begin{aligned}
 R_f &= - \left[\frac{-\frac{g}{\bar{\rho}} \cdot (\overline{\rho' w'})}{\frac{\bar{\epsilon}}{\bar{\rho}} \cdot \frac{\partial \bar{v}}{\partial z}} \right] = - \left[\frac{\frac{g}{c_p \bar{T} \bar{\rho}} (H + 0.61 c_p \bar{T} E)}{\frac{\bar{\epsilon}}{\bar{\rho}} \cdot \frac{\partial \bar{v}}{\partial z}} \right] \\
 &= \frac{g}{\bar{T}} \frac{\left[K_H \frac{\partial \bar{\theta}}{\partial z} + 0.61 \bar{T} K_w \frac{\partial \bar{q}}{\partial z} \right]}{K_m \left[\left(\frac{\partial \bar{u}}{\partial z} \right)^2 + \left(\frac{\partial \bar{v}}{\partial z} \right)^2 \right]}
 \end{aligned}$$

This ratio was effectively the basis of the stability criterion derived by Richardson (1925) in his classical discussion of the rate of growth of turbulence. We usually accept that $K_H = K_M$ and so

$$R_f = \frac{g}{T} \cdot \frac{K_H}{K_M} \left[\frac{\frac{\partial \bar{\theta}}{\partial z} + 0.61 \bar{T} \frac{\partial \bar{q}}{\partial z}}{(\frac{\partial \bar{u}}{\partial z})^2 + (\frac{\partial \bar{v}}{\partial z})^2} \right]$$

All the quantities except K_H and K_M are measurable directly and it is not easy to specify how K_H/K_M will vary with conditions. For these reasons the gradient Richardson number, R_i , is most commonly used, where

$$R_i = \frac{K_M}{K_H} R_f \\ \approx \frac{g}{T} \left[\frac{\frac{\partial \bar{\theta}}{\partial z} + 0.61 \bar{T} \frac{\partial \bar{q}}{\partial z}}{(\frac{\partial \bar{u}}{\partial z})^2 + (\frac{\partial \bar{v}}{\partial z})^2} \right]$$

This is often seen in its simpler form

$$R_i \approx \frac{g}{T} \frac{\partial \bar{\theta} / \partial z}{(\partial \bar{u} / \partial z)^2}$$

| | | |
|----------------|-------------------------------|---|
| $R_i, R_f > 0$ | for stably stratified flow | } |
| $= 0$ | for neutrally stratified flow | |
| < 0 | for unstably stratified flow | |

4. Properties of The Surface-flux Layer

For fuller discussion see, for example, Chap 5,6 of Carson (1976).

4.1 The surface-flux layer.

Adjacent to the surface we can define a layer in which the stress has changed by less than some small percentage from its surface value, i.e. formally we can define a layer such that

$$\frac{|\tau_0 - \tau(z)|}{\tau_0} \leq \epsilon \quad \text{for all } z \text{ in the layer,}$$

where ϵ is some small value, say about 0.1-0.2.

The layer so-defined is often referred to as the constant-stress layer. Unfortunately this terminology can be misleading and it is better to use the more appropriate surface-stress layer. Typically we are dealing with a layer some tens of metres deep.

The definition can be extended to surface-flux layer, in which the turning of the wind with height may be ignored and the vertical fluxes of momentum, heat and water vapour are closely approximated by their surface values (i.e. in this layer they are assumed to be virtually constant with height).

4.2 The Monin-Obukhov Theory.

The Monin-Obukhov similarity hypothesis for the surface-flux layer is the most widely accepted approach for describing the properties of the surface layer. Brought down to the very simplest terms, similarity methods depend on the possibility of being able to express the unknown variables in non-dimensional form, there being suitable argument for saying there exist a length-scale, a velocity-scale (or time-scale) and a temperature (and humidity) scale relevant in doing this. The non-dimensional forms are then postulated to be universal in character and this will hold as long as the scales remain the relevant ones.

The Monin-Obukhov similarity hypothesis for the fully turbulent surface-flux layer (where the Coriolis force is neglected) states that for any transferable property, the distribution of which is homogeneous in space and stationary in time, the vertical flux-profile relation is determined uniquely by the parameters

$$\frac{g}{\bar{T}}, \quad \frac{\tau_0}{\bar{\rho}_0}, \quad \frac{H_0}{\bar{\rho}_0 c_p}, \quad \frac{E_0}{\bar{\rho}_0}$$

which is equivalent to the set (see Section 2.1)

$$\frac{g}{\bar{T}}, \quad u_* , \quad T_* , \quad q_* \quad \left(\psi_* = T_* + 0.61 \bar{T} q_* \right)$$

where g/\bar{T} is the Archimedeian buoyancy parameter.

Instead of using the buoyancy parameter g/\bar{T} it is convenient to use the length-scale, L , uniquely defined by g/\bar{T} , u_* , ψ_* by the relation

$$L = \frac{u_*^2 \bar{T}}{kg \psi_*} = - \frac{u_*^3 \bar{\rho}_0 c_p \bar{T}}{kg [H_0 + 0.61 c_p \bar{T} E_0]}$$

and called the Monin-Obukhov length. L is effectively constant in the surface-flux layer. k is the von Kármán constant (≈ 0.4) and is conventionally introduced solely as a matter of convenience. With upward heat flux taken as positive, L is negative.

Thus L , u_* , T_* , q_* may be taken as the set of basic parameters which uniquely determine the vertical flux-profile relations.

Dimensional analysis leads to flux-gradient relationships expressed in the general form

$$\frac{\partial \bar{s}}{\partial z} = \frac{s_*}{kz} \varphi_s(z/L)$$

where s_* is related to the vertical flux $F_{s,0}$ such that

$$F_{s,0} = \overline{(w's')} = -u_* s_* = -k_s \frac{\partial \bar{s}}{\partial z} = -u_* \frac{kz}{\varphi_s(z/L)} \cdot \frac{\partial \bar{s}}{\partial z}$$

$\varphi_s(z/L)$ are universal functions of z/L only which may be different for each mean transferable property, \bar{s} . The $\varphi_s(z/L)$ have to be established empirically from analysis of surface-layer data.

The profiles themselves are obtained by integrating the above flux-gradient formulae, thus

$$\frac{k (\bar{s}(z) - \bar{s}(z_r))}{s_*} = \int_{\gamma_r}^{\gamma} \frac{\phi_s(\gamma')}{\gamma'} d\gamma' \equiv \bar{\Phi}_s(\gamma, \gamma_r)$$

where $\gamma = z/L$ and $\gamma_r = z_r/L$, where z_r is some reference level at which \bar{s} is known.

The nature of the similarity formulation implies a logarithmic singularity in $\bar{\Phi}_s$ as $z \rightarrow 0$. This is avoided by defining the level z_s as the virtual height at which \bar{s} attains its surface value. For momentum transfer, this level, denoted z_0 , is defined as the virtual height at which $\bar{u} = 0$ and is called the surface roughness length. As stated earlier it is characteristic of the surface and is usually independent of the flow. There are also characteristic 'surface roughness lengths' for heat and water vapour transfer. The problem of discriminating between the surface roughness lengths for the different properties is complex. It remains common practice to use the estimate of z_0 for all three profiles.

Our complete set of profile relationships in the surface layer is :

$$\text{Momentum : } \frac{\partial \bar{u}}{\partial z} = \frac{u_*}{kz} \phi_m(z/L) ; \quad \tau_0 = \bar{\rho}_0 u_*^2 = \bar{\rho}_0 K_m \frac{\partial \bar{u}}{\partial z}$$

$$\text{Sensible heat : } \frac{\partial \bar{\theta}}{\partial z} = \frac{T_*}{kz} \phi_h(z/L) ; \quad H_0 = -\bar{\rho}_0 c_p u_* T_* = -\bar{\rho}_0 c_p K_h \frac{\partial \bar{\theta}}{\partial z}$$

$$\text{Water vapour : } \frac{\partial \bar{q}}{\partial z} = \frac{q_*}{kz} \phi_w(z/L) ; \quad E_0 = -\bar{\rho}_0 u_* T_* = -\bar{\rho}_0 K_w \frac{\partial \bar{q}}{\partial z}$$

Other general relations are :

$$a. \quad K_s = \frac{k u_* z}{\phi_s(z/L)} \quad \text{and therefore } K_s \phi_s = k u_* z \text{ which is independent of } s.$$

$$b. \quad R_i = \frac{z}{L} \cdot \frac{\phi_h(z/L)}{\phi_m^2(z/L)}$$

4.3 The wind profile in the neutral surface-flux layer.

In neutral conditions we find that $\phi_m = 1$ when k is the von Kármán constant (≈ 0.4). Therefore $|L| \rightarrow \infty$, $R_i = 0$, $K_m = k u_* z$

$$\text{and } \frac{\partial \bar{u}}{\partial z} = \frac{u_*}{kz}$$

from which is derived the general well-established logarithmic form of the wind profile for neutral flow in the surface-stress layer,

$$\bar{u}(z) = \frac{u_*}{k} \ln(z/z_0)$$

4.4 Profiles in the non-neutral surface-flux layer.

For a fuller discussion of the empirical forms of ϕ_s in the non-neutral surface layer see, for example, Chap 6 of Carson (1976), Chap 6 of McBean et al (1979) or Chap 2 of Pasquill and Smith (1983).

Fig 10 shows a particular evaluation of ϕ_m and ϕ_h due to Businger et al (1971). The general behaviour is that ϕ_s increases with increasing stability; i.e. decreasing turbulence decreases the mixing and hence increases the normalised vertical gradient of \bar{s} .

Fig 11 illustrates schematically the changing character of the surface-layer wind throughout a clear day and a clear night. For details see, for example, Panofsky and Dutton (1984), Chap 6.

5. Variances of Turbulent Characteristics

5.1 Basic definitions and approximations.

So far we have been concerned with profiles and fluxes. However, many applications depend on the characteristics of the turbulent fluctuations themselves. An important set of variables are the standard deviations of the three wind components. Take u parallel to the mean horizontal wind. By definition then $\bar{v} = 0$ and it is common to assume $\bar{w} = 0$.

The fluctuations θ' of the horizontal wind direction are given approximately (in radians) by

$$\theta' \approx \frac{v'}{\bar{V}}$$

where $\bar{V} = (\bar{u}^2 + \bar{v}^2)^{1/2}$ (often necessarily approximated by \bar{u})

and the fluctuations of the vertical angle, ϕ' , by

$$\phi' \approx \frac{w'}{\bar{V}}$$

These approximations are strictly valid only for small angles, however in practice the errors are usually small.

The variances are defined by

$$\sigma_u^2 = \overline{u'^2}$$

$$\sigma_v^2 = \overline{v'^2} \approx (\bar{V} \sigma_\theta)^2$$

$$\sigma_w^2 = \overline{w'^2} \approx (\bar{V} \sigma_\phi)^2$$

5.2 Variances of the wind components in the neutral surface layer.

Monin-Obukhov similarity theory requires that the standard deviations of the velocity components, normalised by the friction velocity, are functions only of z/L in the surface layer. In neutral conditions the normalised standard deviations should be constants, independent of height or roughness.

This hypothesis is borne out over homogeneous terrain for all the velocity components. Thus

$$\sigma_u = A u_*$$

$$\sigma_v = B u_*$$

$$\sigma_w = C u_*$$

Substitution of u_* from the logarithmic wind profile yields

$$\sigma_u / \bar{V} = \frac{k A}{\ln(z/z_0)}$$

$$\sigma_\theta = \sigma_v / \bar{V} = \frac{k B}{\ln(z/z_0)}$$

$$\sigma_\phi = \sigma_w / \bar{V} = \frac{k C}{\ln(z/z_0)}$$

Note that in the neutral surface layer, σ_u / \bar{V} , σ_θ and σ_ϕ are independent of wind speed and u_* and depend only on z/z_0 (and the respective constants).

Table 2 (from Panofsky and Dutton (1984)) gives a list of estimates of A, B and C from observations over uniform terrain.

5.3 Variances of the wind components in the non-neutral surface layer.

It turns out that of the variances of the three velocity components only σ_w obeys Monin-Obukhov scaling, viz.

$$\sigma_w/u_* = \phi_3(z/L).$$

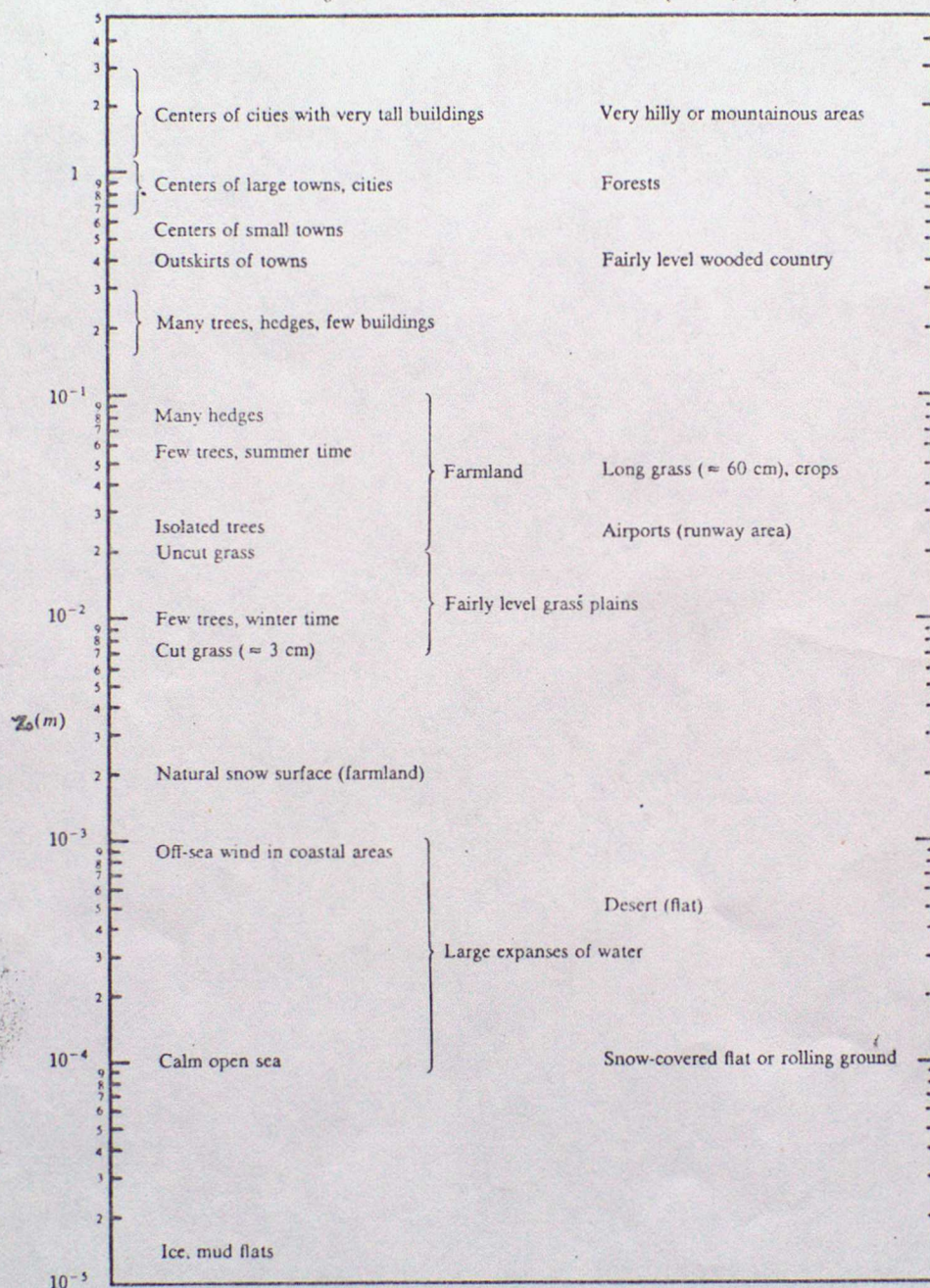
Fig 12 (from Panofsky and Dutton (1984)) illustrates one attempt to determine $\phi_3(z/L)$.

For fuller discussions see, for example, Pasquill and Smith (1983), Chap 2 or Panofsky and Dutton (1984), Chap 7.

REFERENCES

- Businger, J A, Wyngaard, J C, Izumi, Y and Bradley, E F 1971 Flux-profile relationships in the atmospheric surface layer, J Atmos Sci, 28, 181-189
- Carson, D J 1973 The development of a dry inversion-capped convectively unstable boundary layer, Quart J R Met Soc, 99, 450-467
- Carson, D J 1976 The Atmospheric Boundary Layer Introductory Lectures, Met O 20 Tech Note No II/84
- Carson, D J 1982 Current parametrizations of land-surface processes in atmospheric general circulation models, Land Surface Processes in Atmospheric General Circulation Models, Editor P S Eagleson, pp 67-108, CUP
- McBean, G A et al 1979 The Planetary Boundary Layer, WMO Tech Note No 165, Editor G A McBean, WMO-No 530, Geneva
- Panofsky, H A and Dutton, J A 1984 Atmospheric Turbulence. Models and methods for engineering applications. John Wiley and Sons, New York
- Pasquill, F and Smith, F B 1983 Atmospheric Diffusion (Third Edition), Ellis Horwood Ltd, Chichester
- Richardson, L F 1925 Phil Mag, London, 49, p 81
- Smith, F B and Carson, D J 1974 A scheme for deriving day-time boundary-layer wind profiles, Met Mag, 103, 241-255
- Smith, F B and Carson, D J 1977 Some thoughts on the specification of the boundary layer relevant to numerical modelling, Boundary-Layer Meteorol, 12, 307-330

RELATION OF z_0 TO VARIOUS TERRAIN TYPES (ESDU, 1974)



Reprinted with permission.

Table 1. Reproduced from Panofsky and Dutton (1984).

TABLE 2 RATIOS OF STANDARD DEVIATIONS OF VELOCITY COMPONENTS TO FRICTION VELOCITY

| Site | σ_u/u_* | σ_v/u_* | σ_w/u_* |
|--------------------------------|-----------------|-----------------|-----------------|
| <i>Flat Terrain</i> | | | |
| O'Neill, NE | 2.42 | 1.73 | — |
| Sublette, KS | 2.45 | 1.90 | 1.25 |
| Lander, B. C. | 2.20 | 1.90 | 1.40 |
| Beach Island, SC | 2.30 | 1.90 | 1.35 |
| Donaldson, MN | 2.50 | 2.20 | 1.20 |
| Guelph, Ontario ^a | 2.50 | 1.85 | 1.22 |
| St. Louis, MO ^b | 2.39 | 1.79 | 1.26 |
| Roskilde, Denmark ^b | 2.30 | 2.10 | 1.10 |
| Canterbury, NZ | 2.43 | 1.93 | 1.20 |
| Average | 2.39 ± 0.03 | 1.92 ± 0.05 | 1.25 ± 0.03 |
| <i>Rolling Terrain</i> | | | |
| Uppsala, Sweden | 3.2 | — | — |
| Erie, CO | 2.65 | 2.00 | 1.20 |
| Rock Springs, PA | | | |
| Nonmountain | 3.20 | 2.90 | 1.24 |
| Mountain | 4.50 | 3.80 | 1.24 |

^a12–17 min average, no trend removal.

^bRoughness lengths 0.7–1.7 m.

From Panofsky and Dutton (1984)

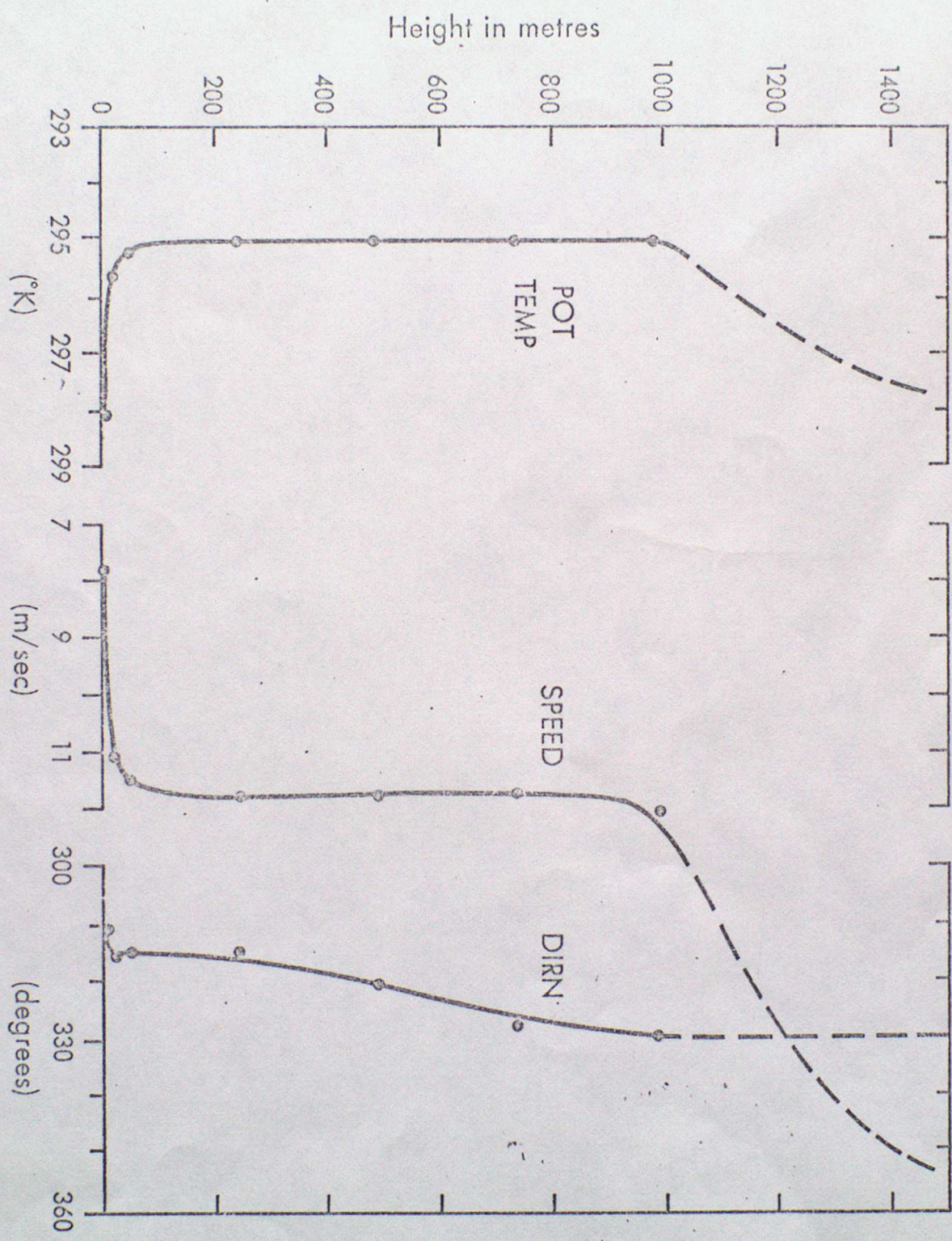


Figure 1. Mean profiles associated with a convective boundary layer

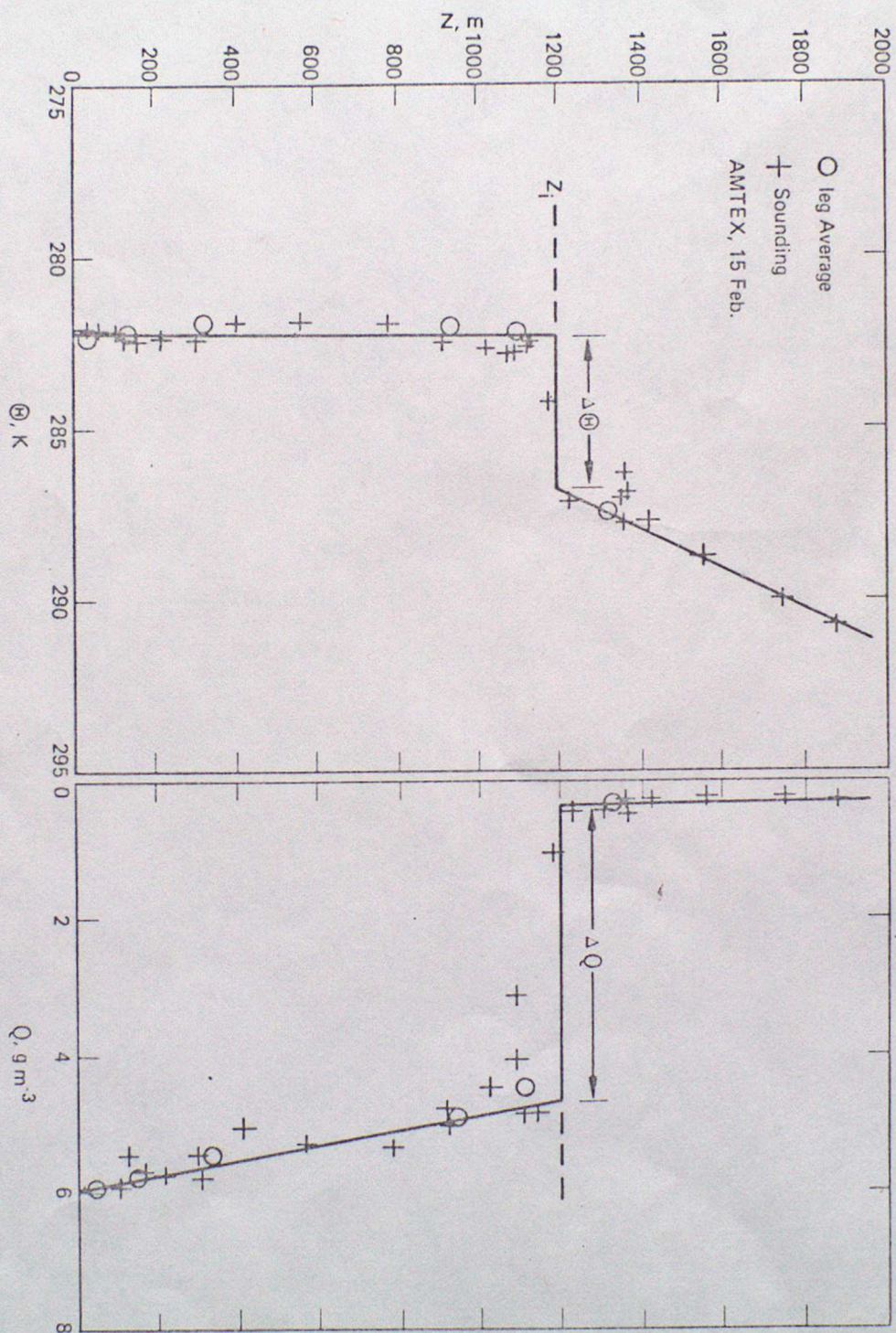


Figure 2 Vertical profiles of mean potential temperature and mean absolute humidity as measured over the sea in the AMTEX experiments. Note the strong jumps in both properties at Z_1 .
(Figure reproduced from McBean et al (1979))

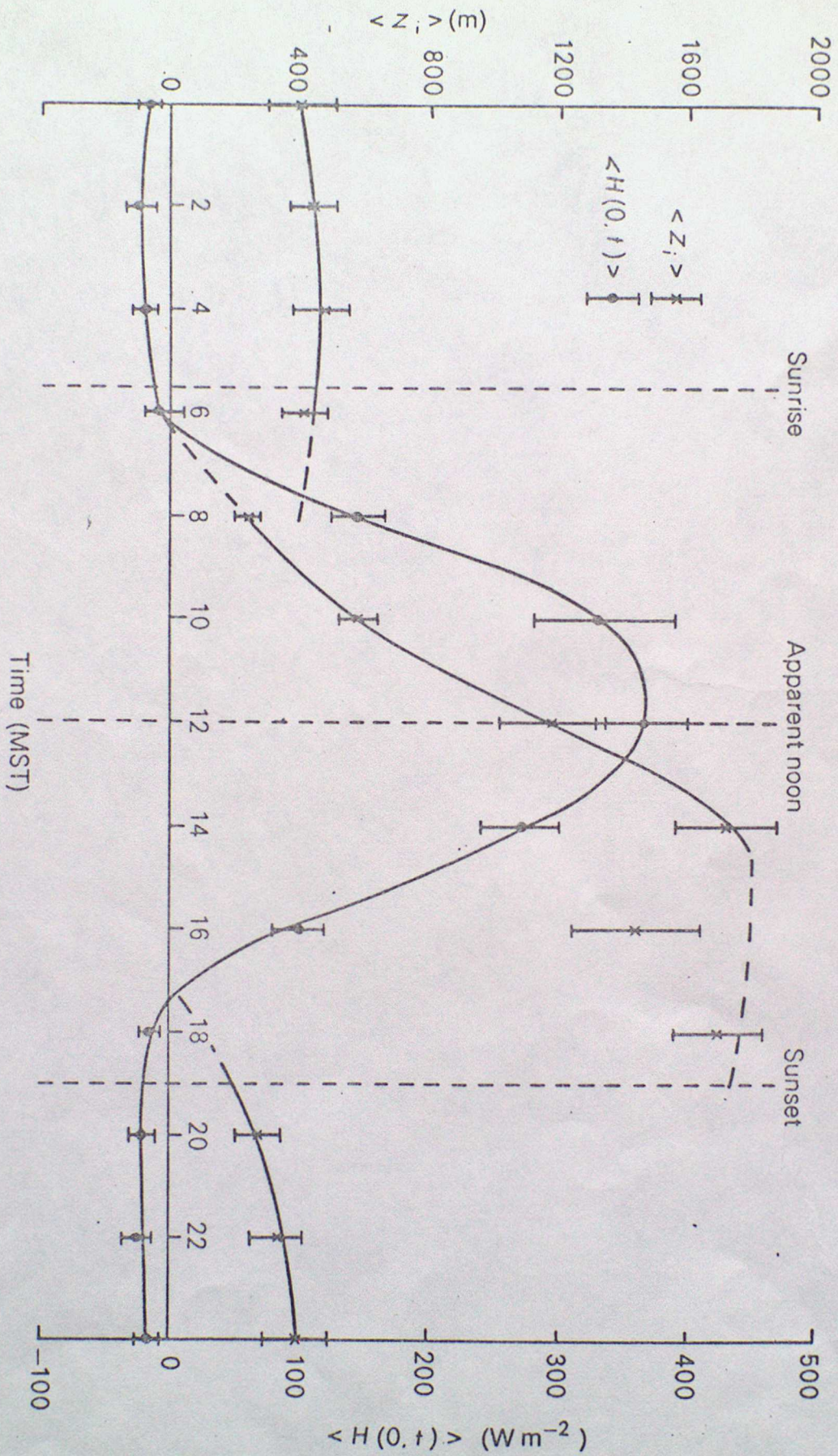


Figure 3. The mean boundary layer thickness, $\langle Z_i \rangle$, and sensible heat flux at the surface, $\langle H(0,t) \rangle$, deduced for the O'Neill data, plotted with standard errors as functions of time of day (Mean Solar Time).
Carson (1973)

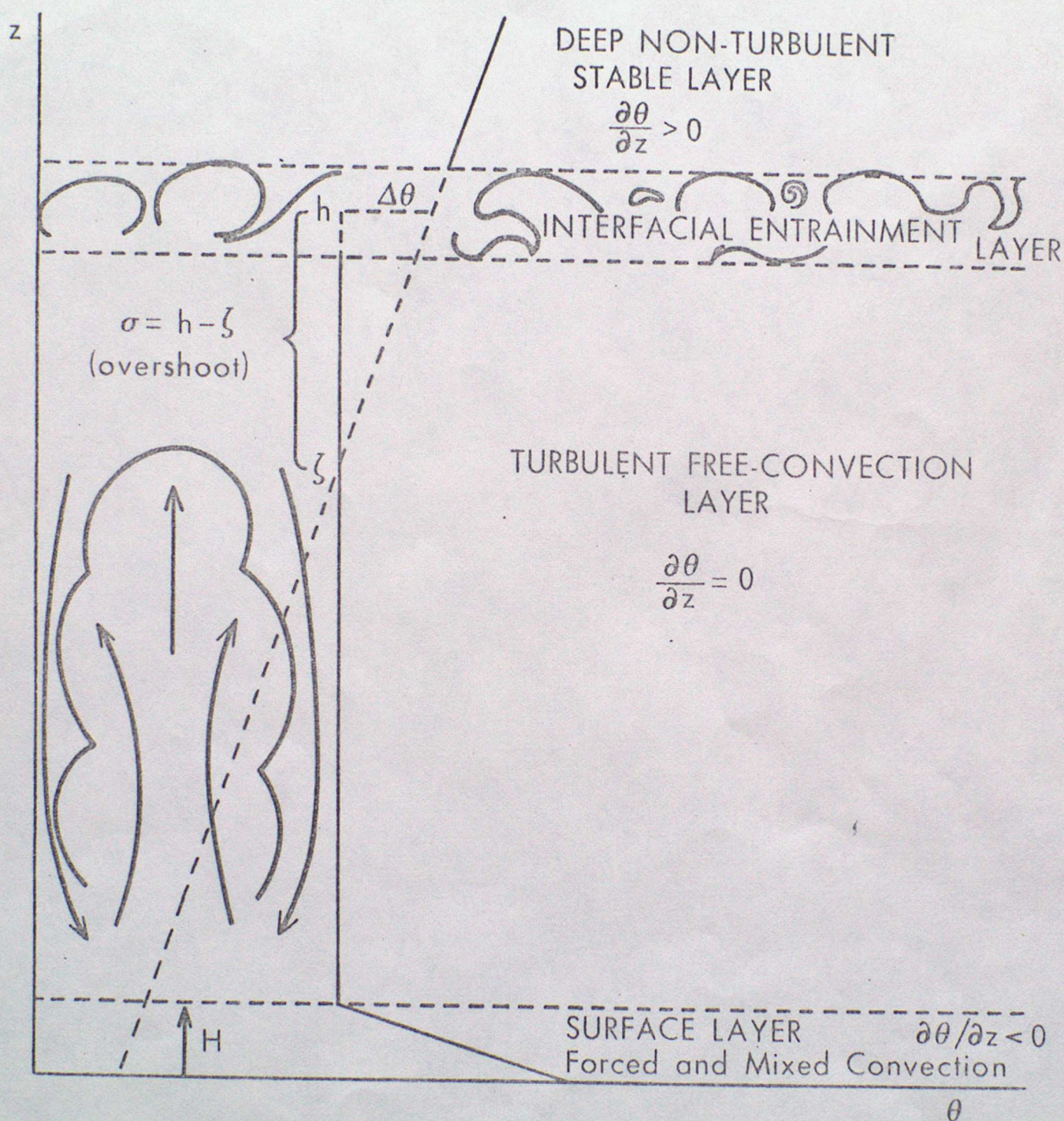


Figure 4. Schematic representation of the developing convectively unstable boundary layer and the adopted potential temperature profile, $\theta(z)$.

Carson (1973)

SCHEMATIC PICTURE OF ENTRAINMENT

WARM
 $\theta = \theta_c + \Delta\theta$

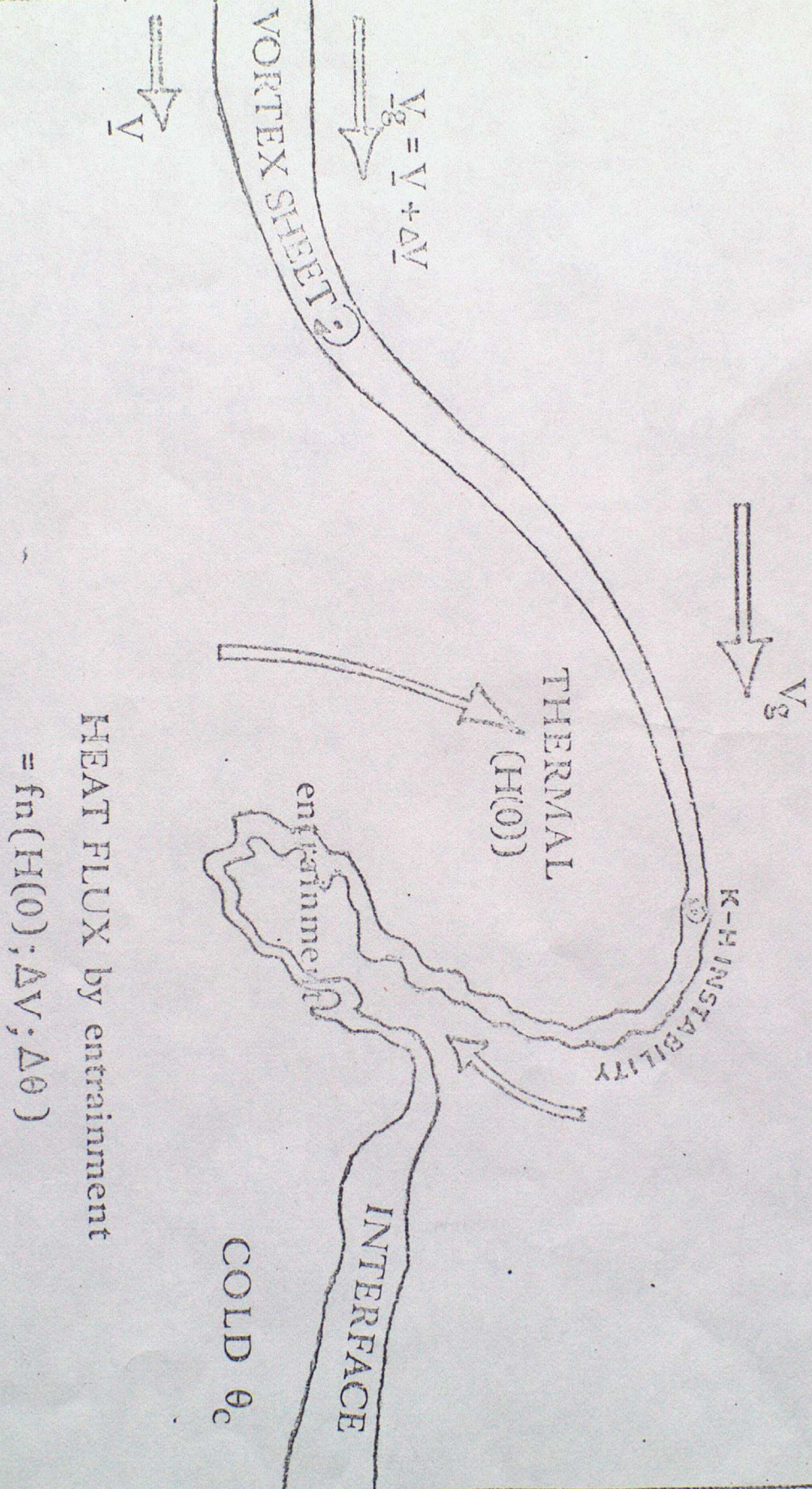


Figure 5. Schematic representation of the mechanisms of entrainment at the top of the boundary layer.

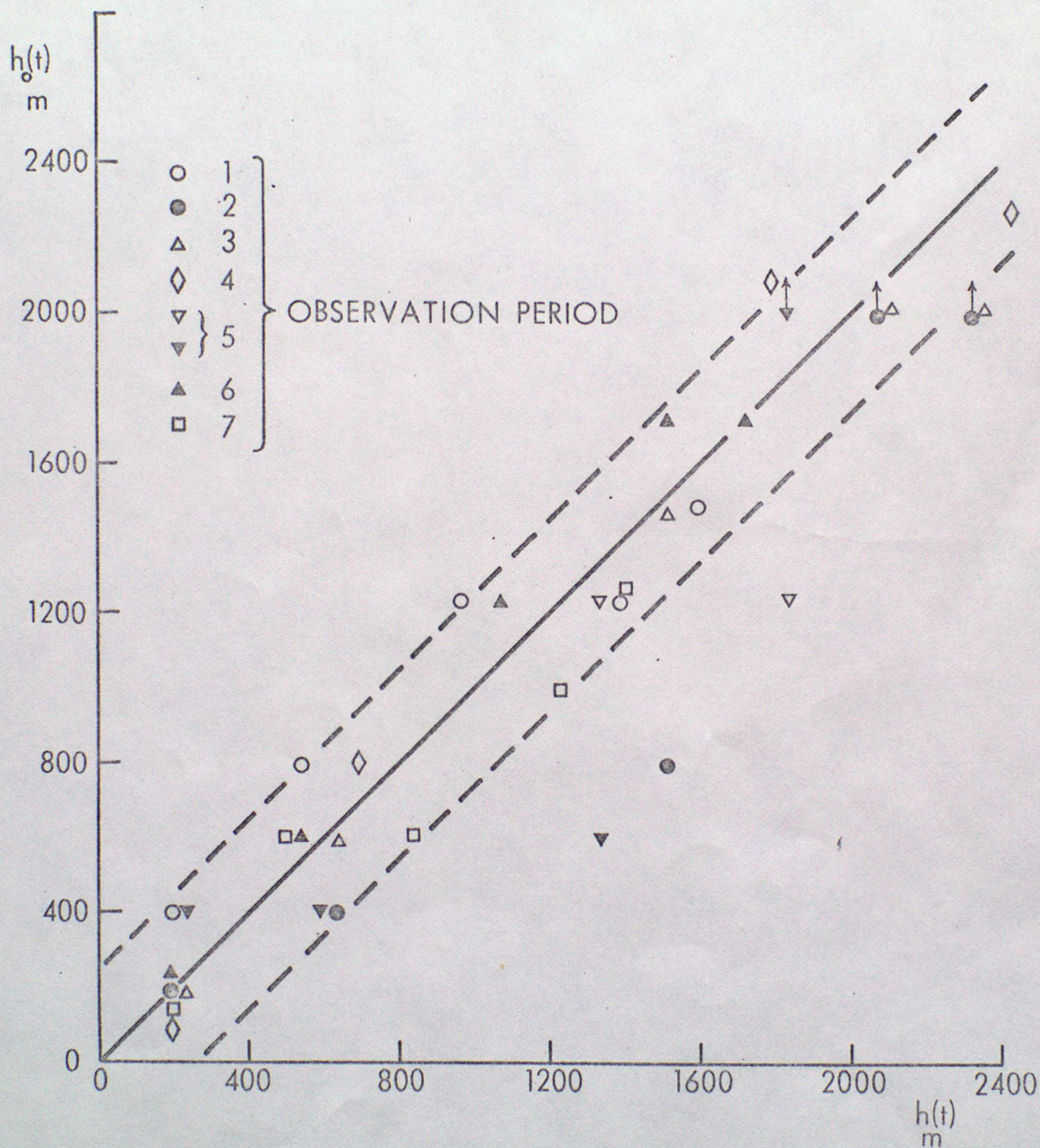


Figure 6 The depth of the O'Neill boundary layer, $h_o(t)$, estimated from profiles, against the depth, $h(t)$, predicted using a three-phase model. The broken lines are $h_o(t) = h(t) \pm 255$ m, where 255 m is the standard error about the line $h_o(t) = h(t)$, the correlation coefficient being 0.93.

Carson (1973)

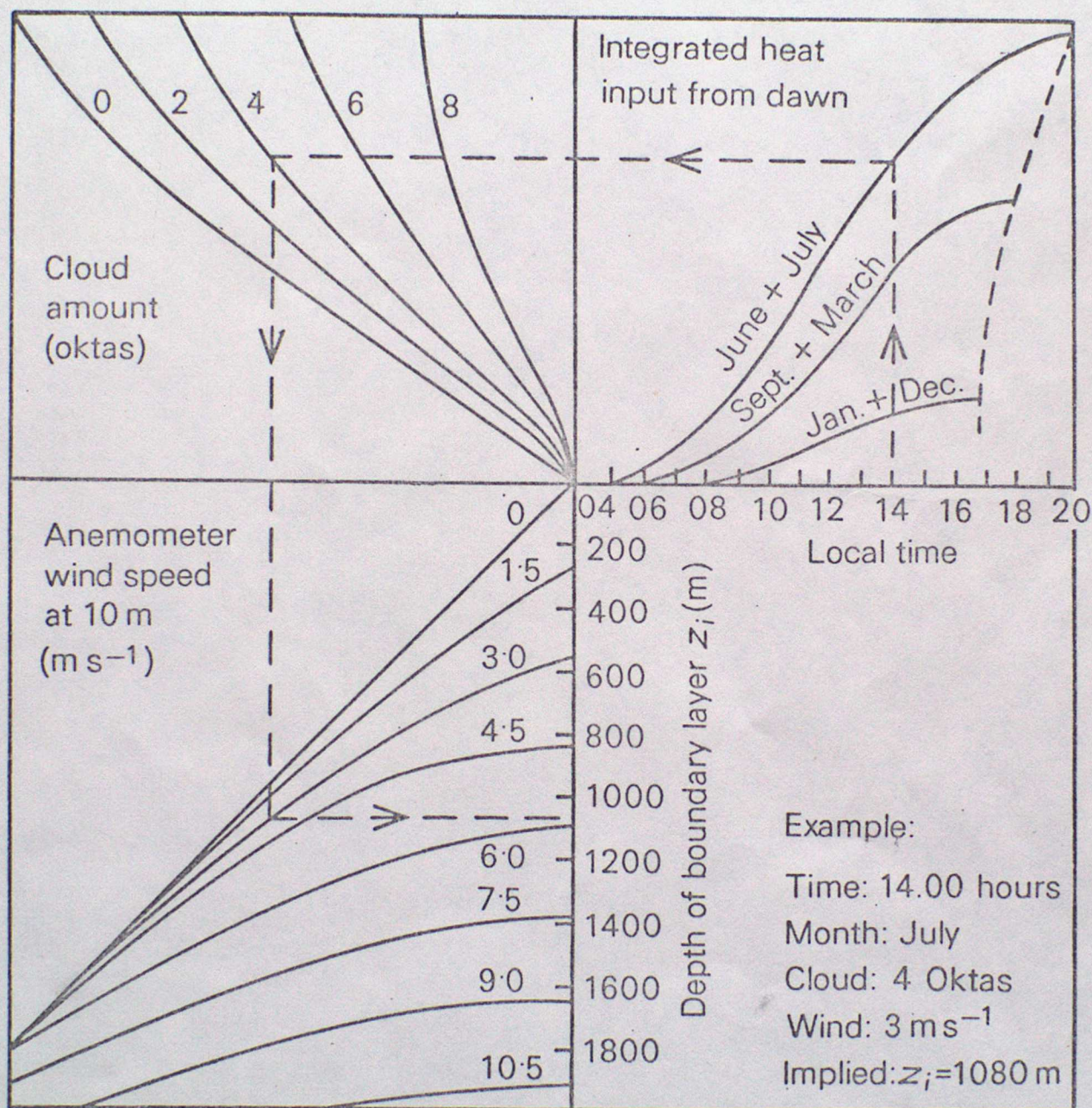


FIGURE 7 A nomogram for estimating the depth of the boundary layer in the absence of marked advective effects or basic changes in weather conditions. The example shows how the diagram is to be used.
 Smith and Carson (1974)

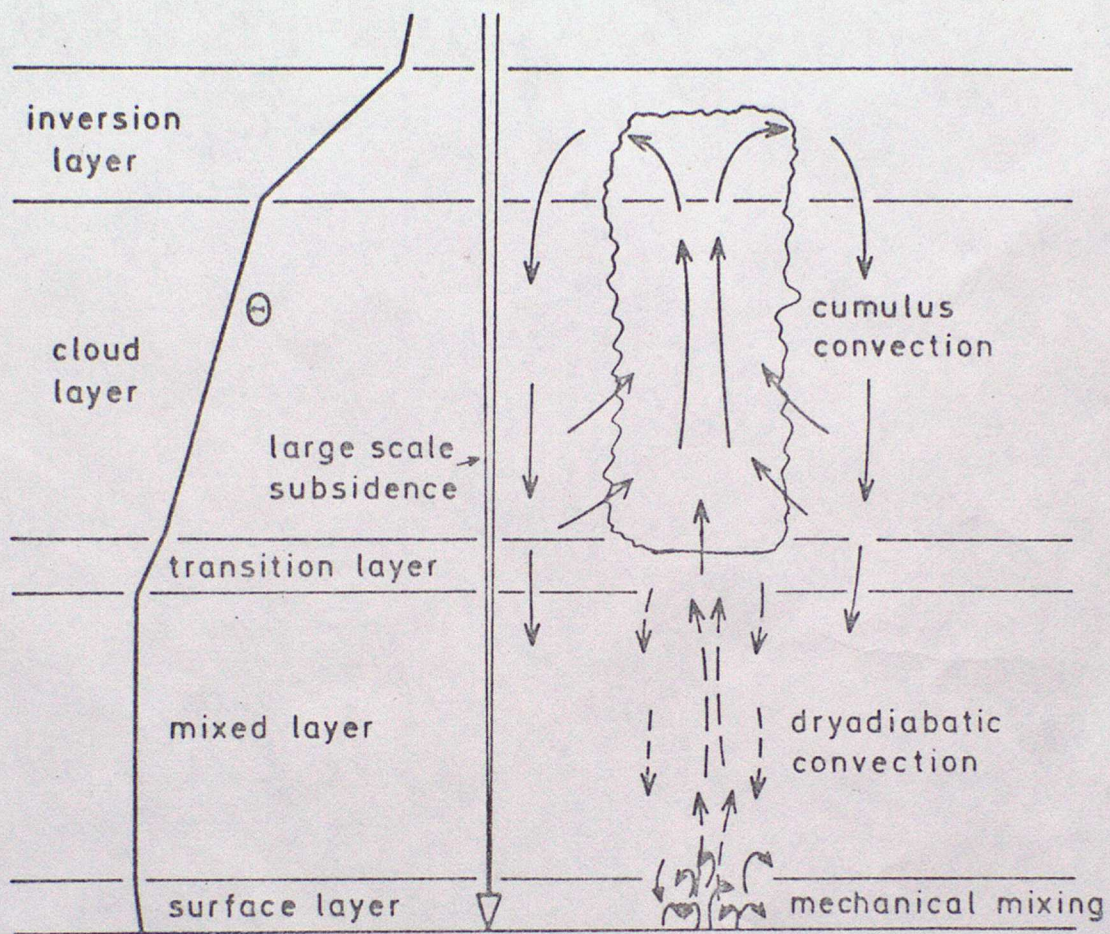
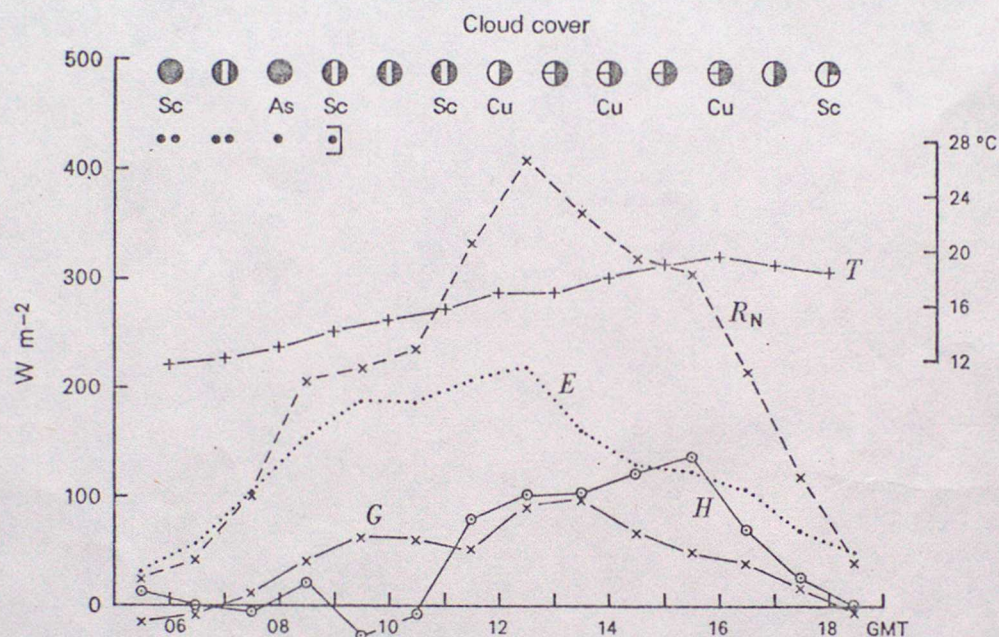
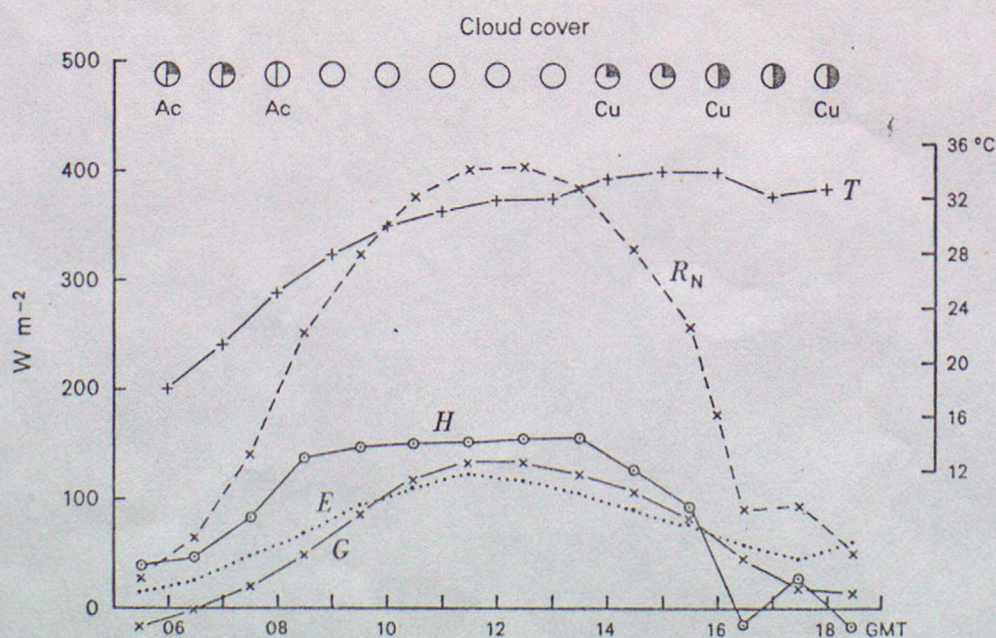


Figure 8. Scheme of dominant processes in a multilayered atmospheric boundary layer. θ = potential temperature.



(a) 20 June 1976



(b) 26 June 1976

Figure 9 Hourly energy budget (06-18 GMT) with cloud cover and screen temperature
 R_N is net radiation, G is soil heat flux, T is screen temperature, E is latent heat flux and H is sensible heat flux.

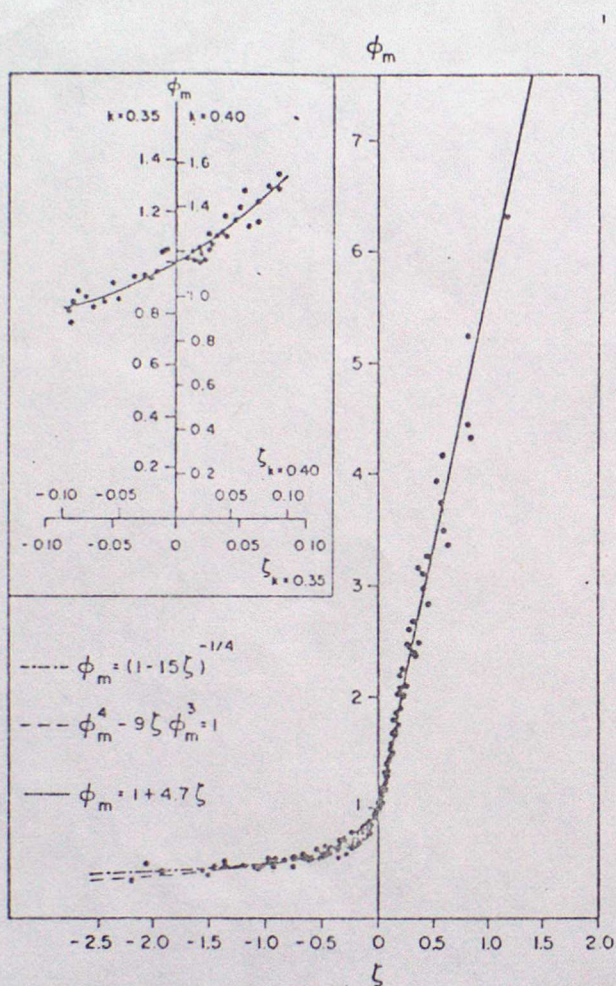


FIG. 1. Comparison of dimensionless wind shear observations with interpolation formulas.

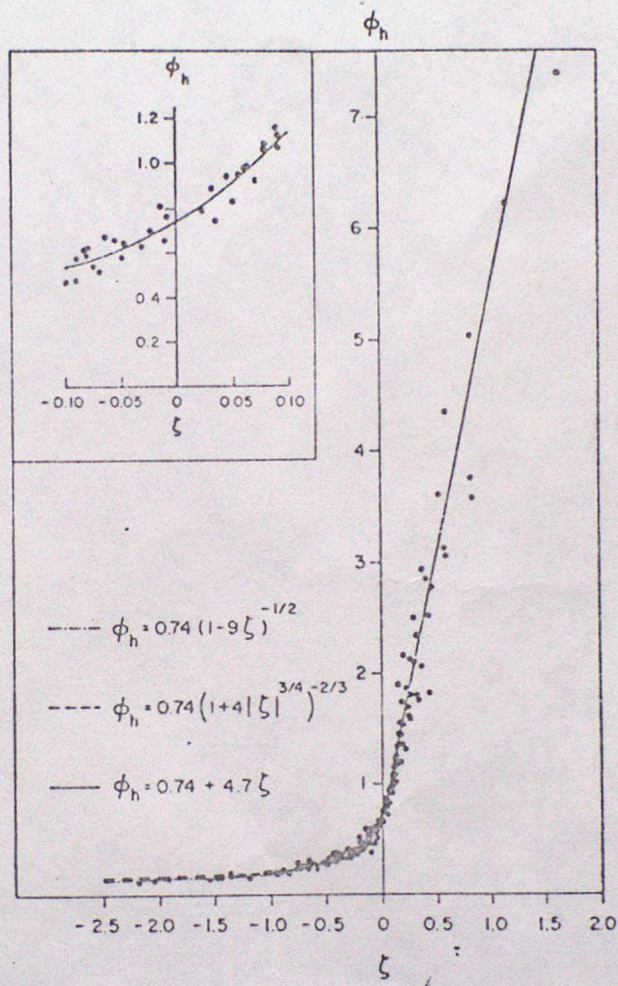


FIG. 2. Comparison of dimensionless temperature gradient observations with interpolation formulas.

Figure 10.

(from Businger, et al., 1971)

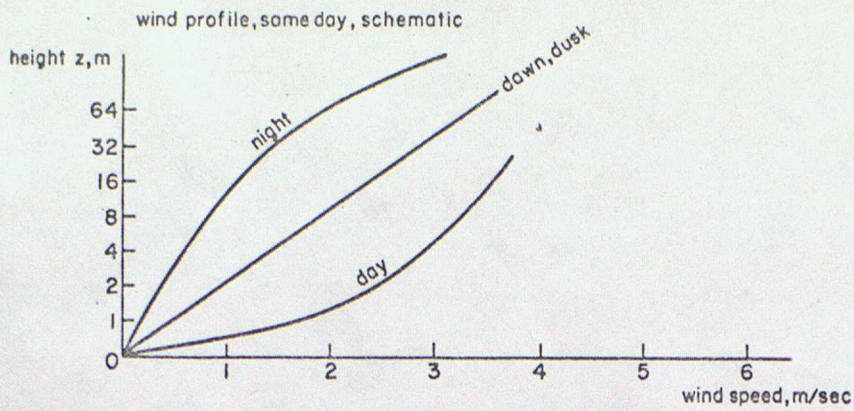


FIGURE 11 • Diurnal variation of wind profiles (schematic).

Panofsky and Dutton (1984)

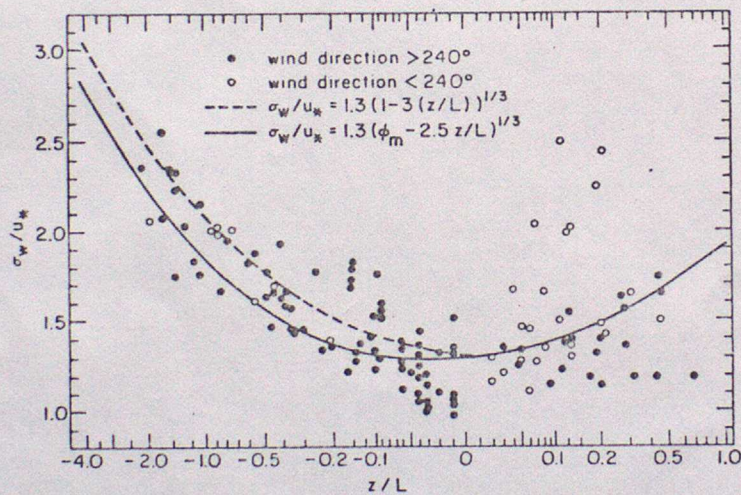


FIGURE 12 σ_w/u_* as a function of z/L at Rock Springs, Pa. below 8 m. Smooth lines represent mathematical fits recommended in the past. For wind direction less than 240° , the air had crossed a low mountain range.

From Panofsky and Dutton (1984)